energy&fuels

Article

pubs.acs.org/EF

New Three-Phase Multicomponent Compositional Model for Asphaltene Precipitation during CO_2 Injection Using CPA-EOS

Hadi Nasrabadi,*[,†] Joachim Moortgat,[‡] and Abbas Firoozabadi[§,∥]

[†]Petroleum Engineering, Texas A&M University, College Station, Texas 77843, United States

[‡]School of Earth Sciences, The Ohio State University, Columbus, Ohio 43210, United States

[§]Reservoir Engineering Research Institute (RERI), Palo Alto, California 94301, United States

[∥]Chemical and Environmental Engineering, Yale University, New Haven, Connecticut 06511, United States

ABSTRACT: Numerical modeling of asphaltene precipitation in petroleum reservoirs is important in relation to possible precipitation around the wellbore in the producing well. Production from some reservoirs results in asphaltene precipitation in the wellbore region, leading to productivity loss and need for cleanup. Fluid injection even when there is asphaltene precipitation may not lead to injectivity loss. There are desirable processes in which precipitation of asphaltenes can lead to "in situ" upgrading of heavy oil recovery. Reservoir compositional models that are currently in use rely on cubic equations of state for asphaltene precipitation. The cubic equations, despite their relative reliability in describing reservoir fluids' phase behavior, become unreliable in asphaltene-rich phase description. A number of noncubic equations of state have been introduced to overcome the shortcomings of cubic equations. The cubic-plus-association equation of state (CPA-EOS) is perhaps the method of choice in representing asphaltenes in compositional modeling. When the hydrocarbon fluids do not contain asphaltenes, CPA-EOS reduces to the standard cubic equation. In this work, we implement CPA-EOS in compositional modeling and introduce a simple technique to speed up considerably the root finding of the CPA-EOS. Our efficient algorithm reduces significantly the additional computational cost from the incorporation of the CPA-EOS. We also derive the basic equations for the total compressibility and total partial molar volume in our implementation of the CPA-EOS compositional modeling. We present three numerical examples for CO_2 injection in 2D and 3D domains saturated with Weyburn oil and show results of asphaltene-rich phase saturation among other predictions. This work introduces a general framework for widespread use of CPA-EOS in compositional modeling in three-phase flows of gas, light liquid, and asphaltene-rich phases.

INTRODUCTION

Asphaltenes are the most polar fraction of crude oil. Their exact chemical structure remains unknown. It is generally accepted that asphaltenes consist of polar polyaromatic material which may contain various metals, oxygen, sulfur, and nitrogen. Asphaltenes are operationally defined as the fraction of crude oil insoluble in normal alkanes such as *n*-pentane but soluble in aromatics such as benzene and toluene at room temperature.[1]

Changes in reservoir pressure (e.g., during primary depletion of highly undersaturated reservoirs) and oil composition (e.g., due to CO_2 injection) can lead to precipitation of an asphaltene phase. Asphaltene precipitation can affect flow in the wellbore in the production well and in the reservoir near the well due to permeability reduction and alteration of rock wettability from water-wet to oil-wet.[2−4]

Despite numerous publications and advances, we are not aware of a three-phase compositional simulator that can treat the asphaltene phase as an asphaltene-rich liquid phase. On the phase behavior side, examples of models for asphaltene precipitation are solubility theory,[5−13] cubic equations of state (EOS),[14−18] colloidal theory,[19] micellization theory,[20−22] McMillan−Mayer−SAFT,[23−25] and perturbed-chain-SAFT.[26−28]

Compositional reservoir simulators are primarily based on cubic EOS to determine the phase separation of hydrocarbon fluids. The EOS method has advantages over solubility theory for modeling asphaltene precipitation. Current compositional simulators mainly use the cubic EOS (e.g., Nghiem et al.[16]). This is motivated by its compatibility with the cubic EOS framework that is widely used for nonasphaltene-related modeling. However, this class of models cannot describe realistic polar−polar interactions relevant to asphaltenes and other polar components, which may obscure the nature of asphaltene precipitation and stabilization.[29] Some of the models take into account the interactions using multiple complex equations or adjustable parameters.[30] These models have high computational cost, which may make their implementation in current compositional simulators unattractive.

Li and Firoozabadi[31] proposed a cubic-plus-association equation of state (CPA-EOS) to study asphaltene precipitation in model solutions (asphaltene + toluene) and heavy oils from the addition of *n*-alkanes. The physical interactions are described by the Peng−Robinson equation of state.[32] The polar−polar interactions between asphaltene molecules and between asphaltene and aromatics/resins (or toluene) molecules are described by the thermodynamic perturbation theory. With this model, they reproduced the experiments for the amount of asphaltene precipitation by different *n*-alkanes from model solutions and seven heavy oils and bitumens over a wide range of temperatures, pressures, and compositions through adjusting only a single parameter. This parameter is the cross-association

Received: December 21, 2015
Revised: February 17, 2016
Published: February 19, 2016

DOI: 10.1021/acs.energyfuels.5b02944
Energy Fuels 2016, 30, 3306−3319

energy between asphaltene and aromatics/resins (or toluene) molecules, which depends on the types of asphaltene and *n*-alkane, and temperature but is independent of pressure and concentration. In a recent investigation Jindrová et al.[33] have shown that while the PR-EOS performs well for solubility of CO_2 and light alkanes in bitumens, when a second liquid phase with high asphaltene content forms, then the PR-EOS becomes unreliable and the CPA-EOS describes the phase behavior in vapor−liquid−liquid equilibria. Zhang et al.[34] compared the performance of the CPA-EOS[31] with the PC-SAFT for asphaltene modeling in six live oils. Their results show that CPA-EOS is more accurate compared to PC-SAFT for modeling asphaltene precipitation over a wide pressure and temperature range.

On reservoir simulation, Mohebbinia et al.[30] implemented PC-SAFT equation of state in a compositional simulation model for predicting asphaltene precipitation during gas injection. As a whole it is desirable to keep the cubic equations of state in compostional modeling due to its simplicity and superiority over the noncubic equations of state and add additional terms when necessary to describe the physics that is not included in the cubic equations of state. This is the basis of our desire to include the CPA-EOS in our work.

In this work, we present the mathematical formulation and an efficient numerical implementation of a three-phase multicomponent compositional model based on the CPA-EOS. The work is organized as follows: we first present the mathematical model governing three-phase compositional flow in porous media and subsequently discuss our numerical scheme based on the mixed finite element and higher-order discontinuous Galerkin methods. We present three examples on the use of our model for simulation of asphaltene precipitation due to CO_2 injection in an oil reservoir. We end the work with concluding remarks.

MATHEMATICAL MODEL

Assumptions. In this work, we neglect the capillary pressure due to low interfacial tension at the conditions of our study. We also ignore Fickian diffusion and mechanical dispersion. Diffusion effect may be negligible in gas injection in unfractured porous media,[35] and diffusion can be very slow in an asphaltene-rich phase. In addition, to the best of our knowledge, diffusion coefficients have not been measured for CO_2−asphaltene mixtures. Mechanical dispersion is generally dominant at high flow rates so we believe, at the conditions of our study, it can be neglected. A recent study[36] shows that for two- and three-phase flow at typical reservoir injection rates, even in the context of viscous and gravitational flow instabilities, the effects of Fickian diffusion and mechanical dispersion are low (because Peclet numbers are generally high).

We assume three phases in our model: (1) asphaltene-rich liquid phase, (2) hydrocarbon-rich liquid phase, and (3) gas phase. We also assume that the reservoir fluid consists of a number of pure hydrocarbon and nonhydrocarbon components (e.g., CO_2, N_2, C_1, C_2, C_3, iC_4, nC_4, iC_5, and nC_5), pseudohydrocarbon components (defined by lumping a number of hydrocarbon components within a certain range in normal boiling points), and a hydrocarbon residue (C_{n+}). In this work, the hydrocarbon residue is split into two components: (1) the "heavy" component that contains the heavy alkanes, the heavy aromatics, and the resins and (2) asphaltene.[29]

The governing equations for isothermal compositional three-phase flow include species-balance equations, Darcy's law, and thermodynamic equilibrium between the phases.

Species-Balance Equations. The species balance for component i is given by

$$\phi \frac{\partial c z_i}{\partial t} + \nabla \cdot \Big(\sum_{\alpha=\mathbf{a},\mathbf{o},\mathbf{g}} c_\alpha x_{i,\alpha} \mathbf{u}_\alpha \Big) = F_i, \quad i = 1, \ldots, n_c \tag{1}$$

F_i may represent the injection and production wells.

The compositions z_i and $x_{i,\alpha}$ are constrained by

$$\sum_{i=1}^{n_c} z_i = \sum_{i=1}^{n_c} x_{i,\alpha} = 1 \tag{2}$$

Darcy's Law. The velocity for each phase ($\mathbf{u}_\alpha$, $\alpha = a, o, g$) is given by Darcy's law:

$$\mathbf{u}_\alpha = \frac{\mathbf{k} k_{r\alpha}}{\mu_\alpha} (\nabla p - \rho_\alpha \mathbf{g}) \tag{3}$$

The viscosities of the asphaltene-rich liquid phase, hydrocarbon-rich liquid phase, and gas phase are a function of temperature, pressure, and phase composition. We use the corresponding-state model[37] to calculate viscosity. Relative permeabilities are functions of phase saturations and are computed using Stone's[38] formulation (see further details in Numerical Results).

Pressure Equation. Based on the concept of volume balance,[39,40] we use the following pressure equation:

$$\phi c_f \frac{\partial p}{\partial t} + \sum_{i=1}^{n_c} \overline{v}_i \Big[\nabla \cdot \Big(\sum_{\alpha=\mathbf{a},\mathbf{o},\mathbf{g}} c_\alpha x_{i,\alpha} \mathbf{u}_\alpha \Big) - F_i \Big] = 0 \tag{4}$$

Thermodynamic Equilibrium. Thermodynamic equilibrium requires the fugacities in the three phases to be equal. We also use phase stability analysis to guarantee the global minimum of Gibbs free energy. In this work, we model asphaltene precipitation as a traditional liquid−liquid or gas−liquid−liquid phase separation. We define equilibrium ratios as $K_{i,g} = x_{i,g}/x_{i,o}$ and $K_{i,a} = x_{i,a}/x_{i,o}$. From the equality of fugacities, we have

$$\ln K_{i,\alpha} = \ln \varphi_{i,o} - \ln \varphi_{i,\alpha}, \quad i = 1, \ldots, n_c; \ \alpha = g, a \tag{5}$$

We also have the following constraint for the molar fractions of each phase (β_α):

$$\sum_{\alpha=g,o,a} \beta_\alpha = 1 \tag{6}$$

where β_α is related to the overall mole fraction of component i (z_i) by

$$z_i = \sum_{\alpha=g,o,a} \beta_\alpha x_{i,\alpha}, \quad i = 1, \ldots, n_c \tag{7}$$

The mass density and molar density of all three phases are obtained from

$$\rho_\alpha = c_\alpha \sum_{i=1}^{n_c} x_{i,\alpha} M_i, \quad \alpha = g, o, a \tag{8}$$

$$c_\alpha = \frac{p}{Z_\alpha R T}, \quad \alpha = g, o, a \tag{9}$$

In this work, Z_α for all the three phases is obtained from the CPA-EOS to take into account the polar−polar interaction (self-association and cross-association) between asphaltene and "heavy" components. Also the calculation of the phase fugacities (in eq 5), the total fluid compressibility, and the total partial molar volume (in eq 4) are based on CPA-EOS. Calculation of the compressibility factor in the CPA-EOS is an important aspect of this work. Our experience shows that efficient and robust calculation of this parameter has direct effect on overall performance of the model. We discuss the calculation steps of this parameter later.

Boundary/Initial Conditions. Appropriate boundary and initial conditions are required to complete the multicomponent three-phase flow formulation. We apply impermeable boundaries at all sides of the domain. We consider a constant oil pressure in the production well (Dirichlet boundary condition) and constant rate in the injection well (Neumann boundary condition).

DOI: 10.1021/acs.energyfuels.5b02944
Energy Fuels 2016, 30, 3306−3319

NUMERICAL MODEL

We solve the species-balance and flow equations using an implicit-pressure−explicit-composition (IMPEC) scheme. We first calculate the pressure and overall composition and then perform phase equilibrium calculations to obtain phase saturations and the species distribution in each phase. We use the mixed finite element (MFE) method to solve the pressure equation (eq 4) and the discontinuous Galerkin (DG) method to solve the species-balance equation (eq 1). Hoteit and Firoozabadi[41−43] provide detailed description of the combined MFE-DG numerical model. This numerical model has been successfully applied and tested for three-phase compositional flow.[44−47] These studies demonstrate powerful features of this combination such as reduction in numerical dispersion and grid orientation effects. In this work, we use the efficient and robust three-phase stability analysis and phase-split routines presented by Li and Firoozabadi.[48]

The main new features of our compositional model are discussed in the following:

Asphaltene-Rich Liquid Phase. While the current compositional simulation models for asphaltene precipitation assume that the precipitated phase is composed of pure asphaltene, in this work, we assume the precipitated phase to consist of various species including the asphaltenes and determine the composition based on three-phase equilibrium computations. Figure 1 provides the composition of an asphaltene-rich phase revealing the presence of various species. The density, viscosity, and other properties of this phase for use in the compositional simulation are part of the computations. The fact that the asphaltene phase is not pure is supported by theoretical analysis and experimental data.[49−51]

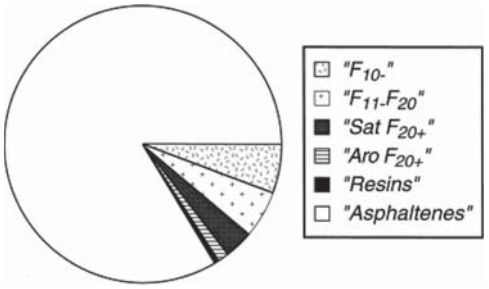

Figure 1. Composition of asphaltene-rich liquid phase[50]

Compressibility Factor. Traditionally in compositional simulation the compressibility factor of each phase (Z_α) is calculated using a cubic equation of state. For example, to obtain Z_α from PR-EOS, one needs to solve the following equation:

$$Z_\alpha = \frac{Z_\alpha}{Z_\alpha - B_\alpha} - \frac{A_\alpha Z_\alpha}{Z_\alpha^2 + 2B_\alpha Z_\alpha - B_\alpha^2} \qquad \alpha = g, o, a \tag{10}$$

where A_α and B_α are functions of pressure, temperature, respective phase compositions, binary interaction parameters, the critical properties, and acentric factors of pure species.[1] In this work, to take into account the polar−polar interaction between asphaltene and resin molecules and between asphaltene molecules themselves, we use CPA-EOS to obtain phase and volumetric properties. In CPA-EOS, eq 10 changes to

$$Z_\alpha = \frac{Z_\alpha}{Z_\alpha - B_\alpha} - \frac{A_\alpha Z_\alpha}{Z_\alpha^2 + 2B_\alpha Z_\alpha - B_\alpha^2} + \frac{4 + 4\eta_\alpha - 2\eta_\alpha^2}{2 - 3\eta_\alpha + \eta_\alpha^2}[x_{a,\alpha}(\chi_{a,\alpha} - 1) + x_{r,\alpha}(\chi_{r,\alpha} - 1)] \qquad \alpha = g, o, a \tag{11}$$

where $\eta_\alpha = B_\alpha/4Z_\alpha$. The subscripts "$a$" and "$r$" represent the asphaltenes and resins/aromatics, respectively. $\chi_{a,\alpha}$ and $\chi_{r,\alpha}$ are the mole fractions of asphaltenes and resins/aromatics in phase α not bonded at one of the association sites, respectively. In this work, we assume association bonding always occurs with an asphaltene molecule on one side and the other side can be either an asphaltene or aromatics/resins molecule.[29] Without the asphaltenes CPA-EOS (eq 11) reduces to the original PR-EOS (eq 10). $\chi_{a,\alpha}$ and $\chi_{r,\alpha}$ in eq 11 are given by[29]

$$\chi_{a,\alpha} = \frac{Z_\alpha}{Z_\alpha + N_a x_{a,\alpha}\chi_{a,\alpha}\Delta^{aa} + N_r x_{r,\alpha}\chi_{r,\alpha}\Delta^{ar}} \qquad \alpha = g, o, a \tag{12}$$

$$\chi_{r,\alpha} = \frac{Z_\alpha}{Z_\alpha + N_a x_{a,\alpha}\chi_{a,\alpha}\Delta^{ar}} \qquad \alpha = g, o, a \tag{13}$$

where $\Delta^{ij} = [1 - 0.5\eta_\alpha/(1-\eta_\alpha)^3]k_{ij}b_{ij}[\exp(\varepsilon_{ij}/k_bT) - 1]$ ($i = a$, $j = a$ or r) represents the "association strength". $b_{ij} = b_i + b_j/2$,, where $b_k = 0.0778\, RT_{ck}/p_{ck}$.[1] k_b is the Boltzmann constant. N_a is the number of identical association sites that each asphaltene molecule has. N_r represents the same parameter for resins/aromatics molecule.

A robust algorithm to find the compressibility factor in the CPA-EOS is through the bisection method which guarantees finding the solution. It is, however, computationally expensive, especially for application in compositional simulation where the compressibility factor needs to be calculated billions of times. Moortgat et al.[45] present an efficient modification of this algorithm based on the Newton method and using the Z-factor from the previous time step as the initial guess. However, they consider the CPA-EOS only for the aqueous phase, which may have only a small fraction of CO_2. This is why, in their work, the initial guess from a previous time step or water density is good enough.

In this work, we used an efficient algorithm based on the classical Newton method where the initial guess is obtained from PR-EOS (eq 10).[52] In our algorithm, we first find the "correct" root of the PR-EOS based on the minimization of the Gibbs free energy.[53] Then, this root will be used as an initial guess for the Newton method. In the CPA-EOS, the compressibility factor comprises physical and association contributions:[53]

$$Z = Z^{physical} + Z^{association} \tag{14}$$

The "correct" root of the cubic EOS (based on the Gibbs free energy minimization) calculates the physical contribution. Therefore, it is relatively close to the final solution that takes into account both the physical and association contributions. In the gas phase, the association part is zero since no asphaltene is present. In the hydrocarbon-rich phase (with very low composition of the asphaltene and resins), the association part is small compared to the physical part and the Newton method converges in a few iterations. In the asphaltene-rich phase, the association part of the compressibility factor can be significant (due to relatively high asphaltene concentration). In our presented examples, even for the asphaltene-rich phase the

DOI: 10.1021/acs.energyfuels.5b02944
Energy Fuels 2016, 30, 3306−3319

Table 1. Fluid Composition, Critical Properties, and Other Relevant Data for the Weyburn Oil[29,61,62]

components	composition (mole fraction)	critical temp (K)	critical pressure (bar)	M_w (g/mol)	acentric factor
CO_2	0.0058	304.14	73.75	44.01	0.2390
$N_2/H_2S/C_1$	0.0575	191.83	47.08	20.66	0.0245
C_2-C_3	0.0774	350.44	44.36	39.89	0.1368
C_4-C_5	0.0619	448.30	35.16	66.72	0.2236
heavy fraction	0.7924	746.22	15.91	220.1	1.0038
asphaltene	0.0050	1474.0	6.342	1800.0	2.0000

Table 2. Non-zero Binary Interaction Coefficients for the Weyburn Oil[29,63] (M_w, Molecular Weight, g/mol)

CO_2–HC	C_1–HC
0.071	$0.0289 + 1.633 \times 10^{-4} M_w$

"correct" root of the PR-EOS provides a good initial guess in the vast majority of the conditions. In the rare occasions in which the Newton method diverges, we switch to the bisection method that always converges but at a relatively high computational cost. In the examples presented in this work, when the bisection method is used for the asphaltene-rich phase, we find only one root for the compressibility factor in the physical range ($Z \geq B$). Our solution for the case in which the bisection method finds more than one root for the CPA-EOS is to calculate the Gibbs free energy for each root and select the one that has a minimum Gibbs free energy. Using the combined Newton–bisection method, we improve the efficiency for the calculation of the compressibility factor by 2 orders of magnitude.

The above modifications in the CPA-EOS are performed at a comparable efficiency with similar calculations using a cubic EOS. The CPU time for one time step using the CPA-EOS (in the examples presented below) is about 3.7 times that of the CPU time for one time step in the PR-EOS when asphaltenes precipitate throughout most of the domain.

Three-Phase Total Compressibility and Partial Molar Volume. Two important parameters in the pressure equation (eq 4) are three-phase total compressibility (c_f) and partial molar volume ($\overline{v_i}$). In this work, we present the calculation of these terms using the CPA-EOS. The details of the derivations are presented in Appendices A–D for completeness.

Formation Damage due to Asphaltene Precipitation. Despite several experimental[54−57] and modeling[58−60] studies on

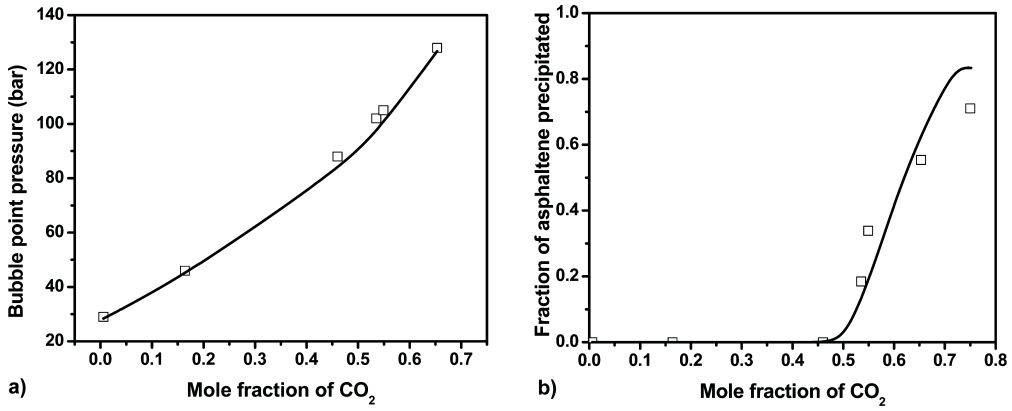

Figure 2. (a) Bubble-point pressure at 332 K and (b) fraction of precipitated asphaltenes at 332 K and 160 bar as a function of CO_2 mole fraction for the Weyburn oil. (Reprinted with permission from ref 29. Copyright 2010 American Chemical Society). Symbols are experimental values,[64] and lines represent calculations by the CPA-EOS.

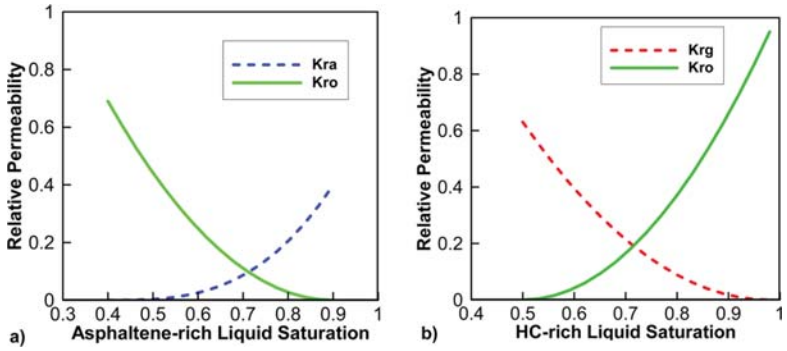

Figure 3. Relative permeability curves for (a) asphaltene-rich liquid/hydrocarbon-rich liquid two-phase system and (b) gas/hydrocarbon-rich liquid two-phase system.

DOI: 10.1021/acs.energyfuels.5b02944
Energy Fuels 2016, 30, 3306−3319

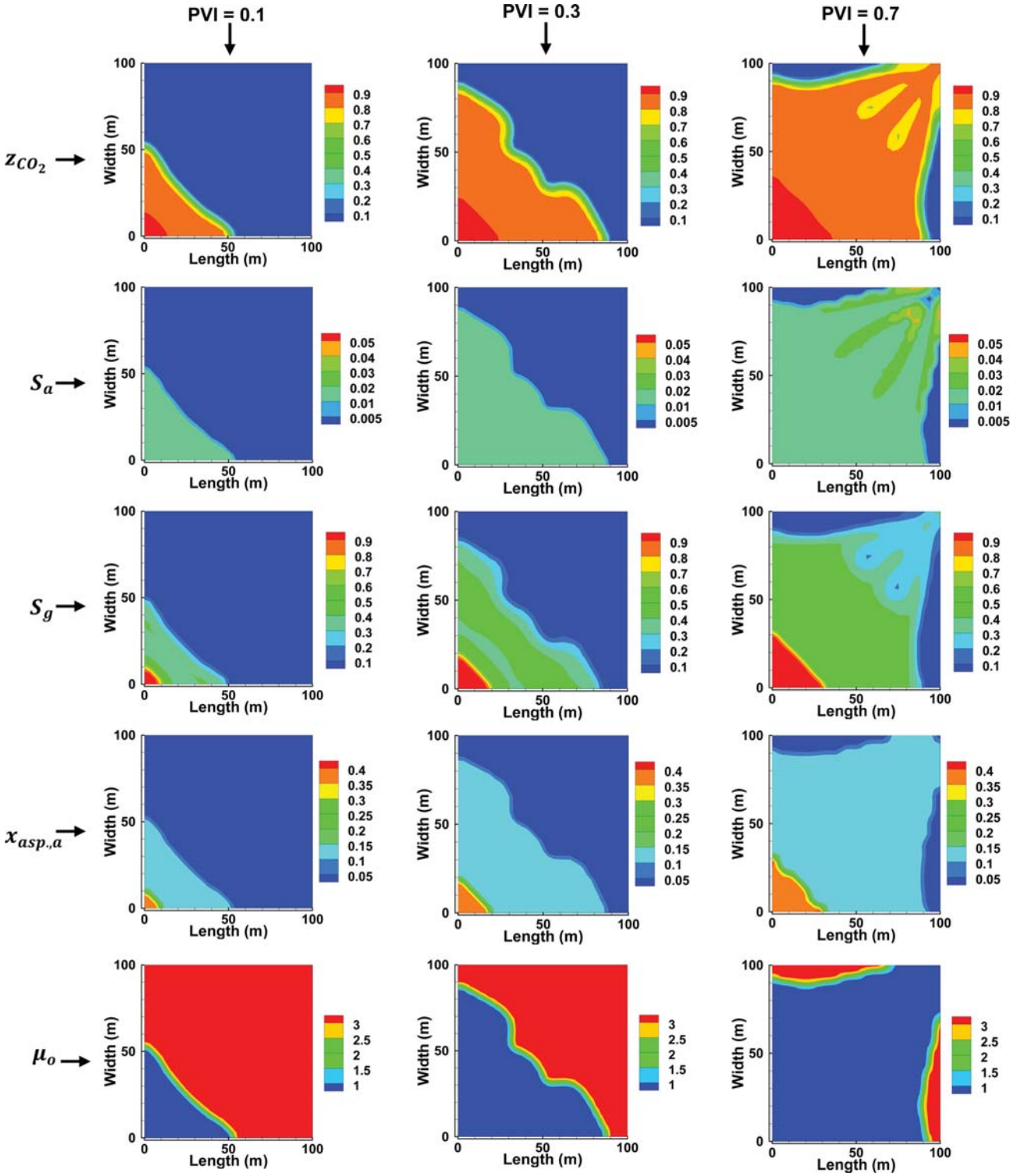

Figure 4. Overall CO_2 composition (z_{CO_2}), asphaltene-rich liquid saturation (S_a), gas saturation (S_g), asphaltene composition in the asphaltene-rich phase ($x_{asp.,a}$), and oil viscosity (μ_o) at different PVI: 2D horizontal domain.

the formation damage caused by asphaltene precipitation, there is significant uncertainty on its underlying mechanisms and quantification. The developed models primarily depend on phenomenological parameters that often have no clear relation to underlying physics. These parameters are therefore difficult to estimate theoretically and are obtained by fitting experimental data. In this work, we use a simple model to take into account the formation damage due to asphaltene precipitation. We alter the relative permeabilities of the hydrocarbon-rich liquid phase and the gas phase based on the saturation of the asphaltene-rich liquid phase. More details of this model are discussed in the following section.

DOI: 10.1021/acs.energyfuels.5b02944
Energy Fuels 2016, 30, 3306−3319

NUMERICAL RESULTS

In this section, we present the following three examples using the new compositional model based on the CPA-EOS for asphaltene precipitation from CO_2 injection in an oil reservoir:

Example 1: 2D Horizontal Domain. In the first example, we consider a 2D horizontal 100 m × 100 m domain. The reservoir temperature is 332 K, and the initial pressure is 160 bar. CO_2 is injected at a constant rate of 0.1 PV/year at the lower left corner. The producer is located at the opposite corner. The pressure at the producing well is set equal to 160 bar. The porosity is 20%, and the permeability is 100 md. We use 32 × 32 grids of dimensions 3.125 m × 3.125 m.

We select the Weyburn oil as the reservoir fluid in this example. Weyburn oil contains a very small amount of light components. Experimental data by Srivastava et al.[64] show that CO_2 injection in this oil leads to asphaltene precipitation. Table 1 lists the fluid composition and the EOS parameters used in the phase behavior calculations. The binary interaction coefficients (BICs) between CO_2 and hydrocarbons and between C_1 and other hydrocarbons are listed in Table 2. Other BICs are set to zero. In Figure 2a, the bubble-point pressure at 332 K is presented for different CO_2/oil mixtures. Figure 2b shows the fraction of precipitated asphaltenes at 332 K and 160 bar as a function of overall concentration of CO_2 in the mixture. As expected, as the CO_2 overall concentration increases, asphaltene precipitation becomes more pronounced. However, at very high CO_2 concentration, the asphaltene phase volume can decrease because of the appearance of a gas phase. This is reflected by the slope decrease in Figure 2b. The CPA-EOS calculations are in good agreement with the measurements.[29] The relevant parameters for the CPA-EOS (eqs 12 and 13) are $N_a = N_r = 4$, $k_{aa} = k_{ar} = 0.01$, $\varepsilon_{aa}/k_b = 2000$ K, and $\varepsilon_{ar}/k_b = 500$ K.

In this example, we have three phases: (1) gas phase, (2) hydrocarbon-rich liquid phase, and (3) asphaltene-rich liquid phase. We use Stone's[38] correlations to model relative permeability of these phases. All two-phase relative permeability curves have a power of 2.0 except for the asphaltene-rich liquid phase with a power of 3.0 (Figure 3). The end-point relative permeability for hydrocarbon-rich liquid with the asphaltene-rich liquid is 0.69. The end-point relative permeability for hydrocarbon-rich liquid with gas is 0.95. The asphaltene-rich liquid has an end-point relative permeability of 0.4, and the end-point relative permeability of gas is 0.63. We assume a critical gas saturation of 2%. The residual saturation for the asphaltene-rich liquid is 40%. The residual saturation of the hydrocarbon-rich liquid to both gas and asphaltene-rich liquid is assumed to be 10%.

Figure 4 presents the profiles for overall CO_2 composition, asphaltene-rich liquid saturation, gas saturation, asphaltene composition (in asphaltene-rich liquid phase), and hydrocarbon-rich liquid viscosity at 0.1, 0.3, and 0.7 pore volumes injected (PVI). This figure shows the CO_2 composition path in the injection process. CO_2 causes various phase behavior effects upon mixing with the crude oil. While the original reservoir fluid mixed with a high fraction of CO_2 stays above the bubble-point pressure (Figure 1a), a CO_2 composition above a mole fraction of 0.45 (Figure 1b) leads to the formation of an asphaltene-rich liquid phase. Continuous increase in CO_2 composition due to further mixing can lead to formation of a gas phase. In this example, the gas phase forms at overall CO_2 molar fractions above approximately 0.73. The gas phase has a CO_2 mole fraction of more than 0.94. One expects to see high gas saturation (due to evaporation of components up to C_{30} in the gas phase) near the injection well and a three-phase gas/hydrocarbon-rich liquid/asphaltene-rich liquid mixture at the mixing zone of CO_2 and crude oil. Next, we further clarify the evolution of the three-phases as CO_2 injection progresses. This figure also shows that, during CO_2 injection, the asphaltene-rich liquid and gas phases form at the mixing zone of CO_2 and crude oil. The asphaltene-rich liquid phase develops across a relatively large fraction of the reservoir. During CO_2 injection, the asphaltene-rich liquid phase first forms near the injection well as CO_2 concentration increases quickly to above the 0.45 mole fraction threshold. However, as the CO_2 concentration increases near the injection well, the saturation of the asphaltene-rich liquid phase becomes relatively constant due to the formation of the gas phase and disappearance of the hydrocarbon-rich liquid phase. As CO_2 injection continues the saturation of gas phase increases. There is also evaporation of lighter components in the asphaltene-rich liquid phase that leads to higher concentration of asphaltene in this phase near the injector (Figure 4).

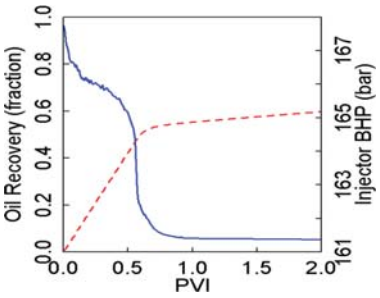

Figure 5. Oil recovery (dashed) and injector bottomhole pressure (solid) vs PVI: 2D horizontal domain.

In CO_2 injection, an area with high saturation of asphaltene-rich liquid phase develops near the producer (Figure 4) from the continuous flow of the asphaltene-rich phase. The following examples show this phenomenon more clearly. Figure 4 shows that the asphaltene-rich liquid saturation stays below the residual saturation (40%) and therefore is immobile. The appearance of this phase is solely due to phase behavior effects. The molar concentration of asphaltene in the asphaltene-rich liquid phase ($x_{asp,a}$) is shown in Figure 4. The highest mole fraction of asphaltene in this phase is 0.38. The initial oil viscosity is 3.0 cP. Dissolution of CO_2 in the crude and reduction in its asphaltene content result in significant reduction in the oil viscosity.

The oil recovery versus PVI and bottomhole pressure at the injector are shown in Figure 5. The oil recovery at breakthrough (0.6 PVI) is 53%. The recovery increases to 60% at 2.0 PVI. The bottomhole pressure at the injector drops after CO_2 breakthrough.

Example 2: 2D Vertical Domain. In this example, we consider a 2D 100 m × 100 m vertical cross-section of the reservoir. The fluid and reservoir properties are set the same as the previous example. CO_2 is injected at the top-right corner of the domain and oil is produced at the bottom-left corner. We use a uniform initial composition (Table 1) and hydrostatic pressure variation (with pressure of 160 bar at the bottom of the formation) for the initial conditions.

Unlike the previous example, gravity affects the CO_2 flow path. Figure 6 shows that most of the injected CO_2 stays at the top of the formation at early times. Similar to the previous example, the asphaltene precipitation occurs throughout a significant portion

DOI: 10.1021/acs.energyfuels.5b02944
Energy Fuels 2016, 30, 3306−3319

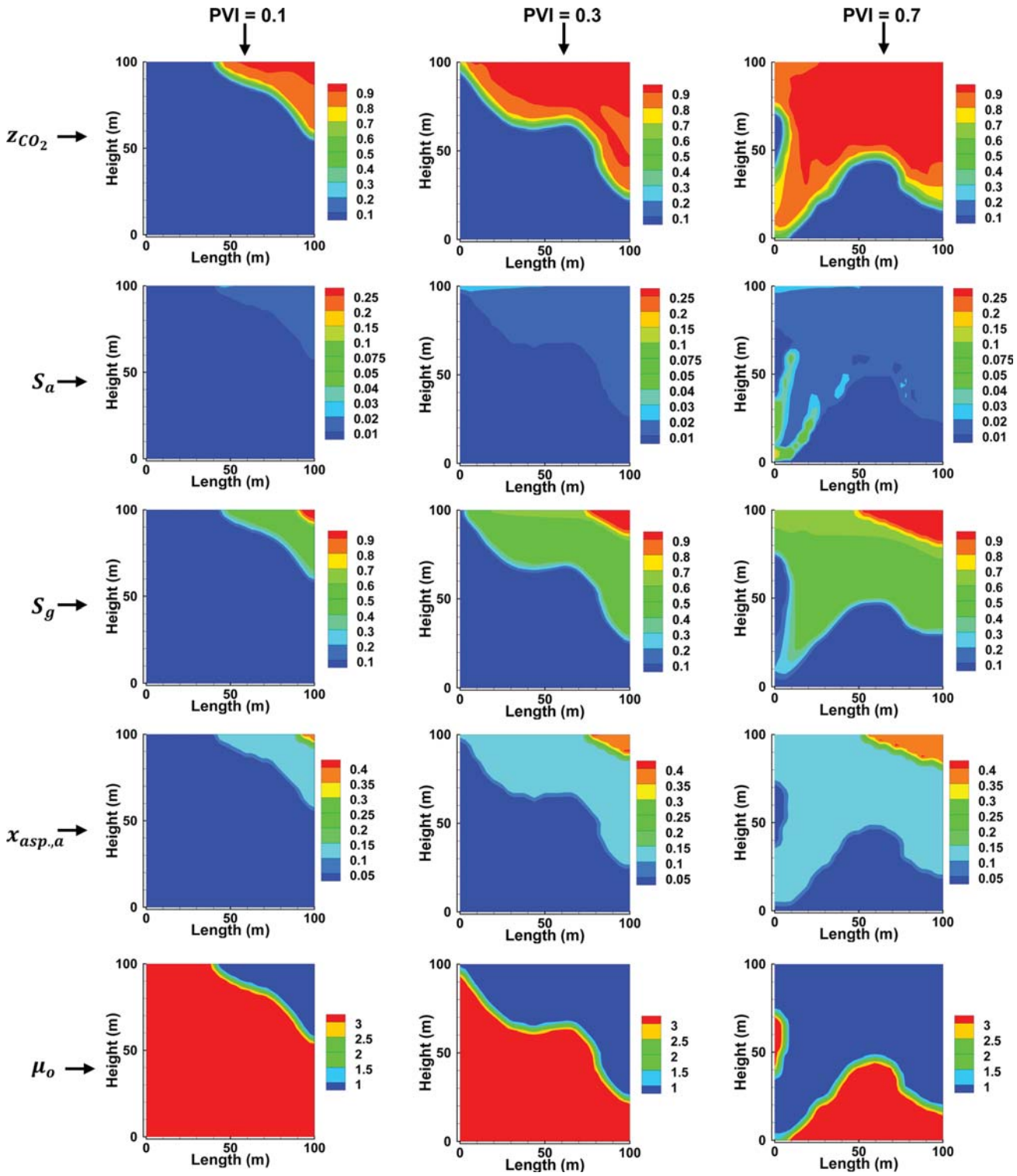

Figure 6. Overall CO_2 composition (z_{CO_2}), asphaltene-rich liquid saturation (S_a), gas saturation (S_g), asphaltene composition in the asphaltene-rich phase ($x_{asp.,a}$), and oil viscosity (μ_o) at different PVI: 2D vertical domain.

of the reservoir due to CO_2 dissolution. However, the saturation of the asphaltene-rich liquid phase stays low except near the production well (Figure 6). At 0.7 PVI, the asphaltene-rich liquid saturation reaches values as high as 20% near the production well. Similar to the previous example, the asphaltene-rich liquid saturation stays low (less than 4%) near the injection well. Figure 6 also presents the gas saturation, composition of asphaltene in asphaltene-rich liquid phase, and oil viscosity at different PVI. Similar trends as in the previous example are observed for these parameters.

Figure 7 presents the oil recovery and bottomhole pressure at the injection well versus PVI. The CO_2 breakthrough occurs at

DOI: 10.1021/acs.energyfuels.5b02944
Energy Fuels 2016, 30, 3306−3319

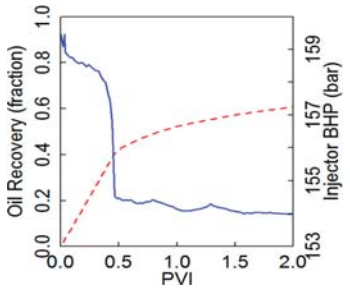

Figure 7. Oil recovery (dashed) and injector bottomhole pressure (solid) vs PVI: 2D vertical domain.

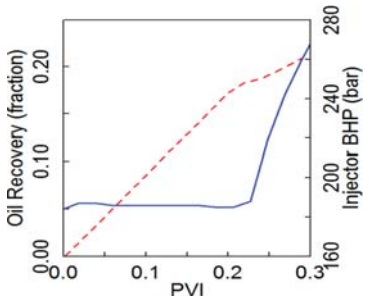

Figure 9. Oil recovery (dashed) and injector bottomhole pressure (solid) vs PVI: 3D domain.

0.46 PVI with approximately 40% oil recovery. The recovery factor increases to roughly 60% after 2.0 PVI.

Example 3: 3D Domain. In this example, we consider a 100 m × 100 m × 40 m domain. We use similar initial and boundary conditions as the 2D examples. The injector is located at the top-left corner and the producer is on the bottom-right corner. We use 32 × 32 × 20 grids of dimensions 3.125 m × 3.125 m × 2.5 m in *x*, *y*, and *z* directions, respectively. Similar to the 2D examples, the permeability is 100 md and the porosity is 20%. The 3D example allows features of asphaltene deposition in the production well due to asphaltene-rich phase buildup to high saturations and subsequent oil rate reduction. In our example, because of the fixed injection rate and constant pressure at the production well, the injection pressure may increase significantly.

Figure 8 displays the variation in overall CO_2 composition and asphaltene-rich liquid saturation at PVI = 0.3. This figure shows that CO_2 flows, due to gravity, mainly at the top of the reservoir. Due to CO_2 dissolution, an asphaltene-rich liquid saturation forms. The asphaltene-rich phase saturation stays low near the injector similar to our 2D results. The asphaltene-rich saturation near the producer is much higher (about 40%) than in the 2D examples. This high saturation of precipitated asphaltene phase causes a significant increase in the injection pressure as shown in Figure 9. The injection pressure increases more than 80 bar (1160 psi) after 0.3 PVI. We stopped the simulation at 0.3 PVI due to this high pressure.

Figure 9 shows an early breakthrough after approximately 0.2 PVI. The recovery factor at breakthrough is 0.18. There is a slight increase in injection pressure at the beginning due to formation of asphaltene-rich liquid phase near the injector. The pressure does not increase further at that point due to small saturation of the asphaltene-rich liquid phase (about 4%). However, due to the high saturation of the asphaltene-rich phase at the producer the bottomhole pressure increases significantly. At this stage there is need to clean up the well.

CONCLUSIONS

The central theme of this work is the presentation of a new three-phase multicomponent compositional model for asphaltene precipitation using CPA-EOS. In this work, we discuss for the first time a unified compositional framework to model all three phases: gas, hydrocarbon-rich liquid, and asphaltene-rich liquid. We allow all components to be present in the asphaltene-rich (and other) phases, unlike simplified models in which the asphaltene phase consists of only the asphaltene component. Therefore, the phase behavior of *all* phases changes when asphaltenes precipitate, in agreement with experimental observations. An efficient algorithm for the calculation of the compressibility factor in the CPA-EOS reduces the computational cost for phase behavior calculations significantly. The outcome is an efficient CPA-EOS compositional model with comparable performance to conventional compositional models based on the cubic EOS.

We use our model to evaluate the extent of asphaltene precipitation from CO_2 injection in an oil reservoir. The reservoir is saturated with Weyburn oil, prone to asphaltene precipitation when mixed with CO_2. Our results show that the asphaltene-rich liquid phase will form in a relatively large volume of the reservoir due to CO_2/oil mixing. The asphaltene-rich liquid saturation close to the injection well reaches a maximum and stops to increase as more CO_2 is injected. The most significant accumulation of the asphaltene-rich liquid phase is around the production well. This accumulation, in our 3D example, led to significant increase in injection pressure. When the injection pressure is not allowed to increase there will be a decrease in production rate due to asphaltene-rich phase accumulation in the wellbore region of the producer.

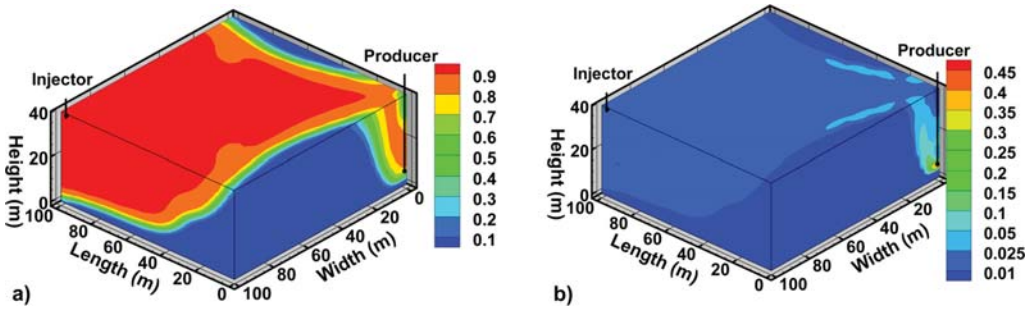

Figure 8. (a) overall CO_2 composition and (b) asphaltene-rich liquid saturation at PVI = 0.3: 3D domain.

DOI: 10.1021/acs.energyfuels.5b02944
Energy Fuels 2016, 30, 3306−3319

APPENDIX A: THREE-PHASE TOTAL FLUID COMPRESSIBILITY

The equations used to calculate three-phase total fluid compressibility from the CPA-EOS are presented in this Appendix:[1]

$$c_f = -\frac{1}{V_T}\left(\frac{\partial V_T}{\partial p}\right)_{T,\mathbf{n}} \tag{A-1}$$

where

$$V_T = \sum_{\alpha=g,o,a} V_\alpha = \frac{RT}{p}\sum_{\alpha} Z_\alpha n_\alpha \tag{A-2}$$

From (A-2), we have

$$\left(\frac{\partial V_T}{\partial p}\right)_{T,\mathbf{n}} = -\frac{RT}{p^2}\sum_{\alpha=g,o,a} Z_\alpha n_\alpha + \frac{RT}{p}\sum_{\alpha=g,o,a}\left[n_\alpha\left(\frac{\partial Z_\alpha}{\partial p}\right)_{T,\mathbf{n}} + Z_\alpha\left(\frac{\partial n_\alpha}{\partial p}\right)_{T,\mathbf{n}}\right] \tag{A-3}$$

Therefore, to calculate the total compressibility, one needs to calculate $(\partial Z/\partial p)_{T,\mathbf{n}}$ and $(\partial n/\partial p)_{T,\mathbf{n}}$. We first present the steps to calculate $(\partial n_\alpha/\partial p)_{T,\mathbf{n}}$ and then $(\partial Z_\alpha/\partial p)_{T,\mathbf{n}}$. We have

$$\left(\frac{\partial n_\alpha}{\partial p}\right)_{T,\mathbf{n}} = \sum_{i=1}^{n_c}\left(\frac{\partial n_{i,\alpha}}{\partial p}\right)_{T,\mathbf{n}} \qquad \alpha = g,\ o,\ a \tag{A-4}$$

where $n_{i,\alpha}$ is the number of moles of component i in phase α. To calculate $(\partial n/\partial p)_{T,\mathbf{n}}$, we have $3n_c$ unknowns in eq A-4. We need $3n_c$ equations to find these unknowns. Material balance yields

$$n_i = \sum_{\alpha=g,o,a} n_{i,\alpha} \qquad i = 1,\ ...,\ n_c \tag{A-5}$$

where n_i is the total number of moles of component i in the three-phase system that is constant. Therefore, from eq A-5 we have the following n_c equations:

$$\sum_{\alpha=g,o,a}\left(\frac{\partial n_{i,\alpha}}{\partial p}\right)_{T,\mathbf{n}} = 0 \qquad i = 1,\ ...,\ n_c \tag{A-6}$$

The remaining $2n_c$ equations come from the following equilibrium conditions:

$$\left(\frac{\partial f_{i,g}}{\partial p} - \frac{\partial f_{i,o}}{\partial p}\right)_{T,\mathbf{n}} = \left(\frac{\partial f_{i,o}}{\partial p} - \frac{\partial f_{i,a}}{\partial p}\right)_{T,\mathbf{n}} = 0 \qquad i = 1,\ ...,\ n_c \tag{A-7}$$

where $f_{i,\alpha}(\alpha = g,\ o,\ a)$ is the fugacity of component i in phase α. The calculation of this parameter using CPA-EOS is explained in Appendix C. One can write eq A-7 as

$$\left[\sum_{k=1}^{n_c}\left(\frac{\partial f_{i,g}}{\partial n_{k,g}}\right)_{T,\mathbf{n}_{g,k}}\left(\frac{\partial n_{k,g}}{\partial p}\right)_{T,\mathbf{n}} - \sum_{k=1}^{n_c}\left(\frac{\partial f_{i,o}}{\partial n_{k,o}}\right)_{T,\mathbf{n}_{o,k}}\left(\frac{\partial n_{k,o}}{\partial p}\right)_{T,\mathbf{n}}\right] + \left[\left(\frac{\partial f_{i,g}}{\partial p}\right)_{\mathbf{n}_g} - \left(\frac{\partial f_{i,o}}{\partial p}\right)_{\mathbf{n}_o}\right] = 0 \qquad i = 1,\ ...,\ n_c \tag{A-8}$$

$$\left[\sum_{k=1}^{n_c}\left(\frac{\partial f_{i,o}}{\partial n_{k,o}}\right)_{T,\mathbf{n}_{o,k}}\left(\frac{\partial n_{k,o}}{\partial p}\right)_{T,\mathbf{n}} - \sum_{k=1}^{n_c}\left(\frac{\partial f_{i,a}}{\partial n_{k,a}}\right)_{T,\mathbf{n}_{a,k}}\left(\frac{\partial n_{k,a}}{\partial p}\right)_{T,\mathbf{n}}\right] + \left[\left(\frac{\partial f_{i,o}}{\partial p}\right)_{\mathbf{n}_o} - \left(\frac{\partial f_{i,a}}{\partial p}\right)_{\mathbf{n}_a}\right] = 0 \qquad i = 1,\ ...,\ n_c \tag{A-9}$$

The calculation steps for $(\partial f_i/\partial n_k)_{T,\mathbf{n}_k}$ and $(\partial f_i/\partial p)_{\mathbf{n}}$ using the CPA-EOS are reported in Appendix C.

To calculate $(\partial Z_\alpha/\partial p)_{T,\mathbf{n}}$ $(\alpha = g,\ o,\ a)$, we use the following equation:

$$\left(\frac{\partial Z_\alpha}{\partial p}\right)_{T,\mathbf{n}} = \left(\frac{\partial Z_\alpha}{\partial p}\right)_{T,\mathbf{n}_\alpha} + \sum_{k=1}^{n_c}\left(\frac{\partial Z_\alpha}{\partial n_{\alpha,k}}\right)_{T,\mathbf{n}_{\alpha,k}}\left(\frac{\partial n_{\alpha,i}}{\partial p}\right)_{T,\mathbf{n}_\alpha} \qquad \alpha = g,\ o,\ a \tag{A-10}$$

The calculation steps for $(\partial Z_\alpha/\partial_p)_{T,\mathbf{n}_\alpha}$ and $(\partial Z_\alpha/\partial n_{\alpha,k})_{T,\mathbf{n}_{\alpha,k}}$ using the CPA-EOS is explained in Appendix D.

APPENDIX B: THREE-PHASE PARTIAL MOLAR VOLUME

The calculation steps for three-phase partial molar volume are presented in this section. Partial molar volume of component i $(\overline{v_i})$ is defined as

$$\overline{v_i} = \left(\frac{\partial V_T}{\partial n_i}\right)_{T,p,\mathbf{n}_i} = \sum_{\alpha=g,o,a}\left[\sum_{k=1}^{n_c}\left[\frac{Z_\alpha RT}{p} + \frac{n_\alpha RT}{p}\left(\frac{\partial Z_\alpha}{\partial n_{k,\alpha}}\right)_{T,p,\mathbf{n}_{\alpha,k}}\right]\left(\frac{\partial n_{k,\alpha}}{\partial n_i}\right)_{T,p,\mathbf{n}_{\alpha,i}}\right] \qquad i = 1,\ ...,\ n_c \tag{B-1}$$

To calculate partial molar volume from the above equation, one needs to find $3n_c$ unknown values of $(\partial n_{k,\alpha}/\partial_{n_i})_{T,p,\mathbf{n}_{\alpha,i}}(\alpha = g,\ o,\ a)$. Similar to calculation of total fluid compressibility, the following material balance and equality of fugacities (due to equilibrium) provide the required $3n_c$ equations:

$$\sum_{\alpha=g,o,a}\left(\frac{\partial n_{i,\alpha}}{\partial n_i}\right)_{T,p,\mathbf{n}_{\alpha,i}} = 0 \qquad i = 1,\ ...,\ n_c \tag{B-2}$$

$$\left(\frac{\partial f_{i,g}}{\partial n_i} - \frac{\partial f_{i,o}}{\partial n_i}\right)_{T,p,\mathbf{n}_{\alpha,i}} = \left(\frac{\partial f_{i,o}}{\partial n_i} - \frac{\partial f_{i,a}}{\partial n_i}\right)_{T,p,\mathbf{n}_{\alpha,i}} = 0 \qquad i = 1,\ ...,\ n_c \tag{B-3}$$

APPENDIX C: EXPRESSIONS OF $(\partial f_i/\partial n_k)_{T,n_k}$ AND $(\partial f_i/\partial p)_{\mathbf{n}}$ FROM CPA-EOS

To calculate three-phase total compressibility and three-phase partial molar volume, we need to calculate f_i, $(\partial f_i/\partial n_k)_{T,\mathbf{n}_k}$ and $(\partial f_i/\partial_p)_{\mathbf{n}}$ for each phase using the CPA-EOS. The expressions for these parameters are presented in this Appendix. To calculate f_i, we have

DOI: 10.1021/acs.energyfuels.5b02944
Energy Fuels 2016, 30, 3306−3319

$$\ln \varphi_i = -\ln(Z-B) + \frac{B_i}{B}\left(\frac{B}{Z-B} - \frac{AZ}{Z^2+2BZ-B^2}\right) - \frac{A}{2\sqrt{2}B}\left(\frac{2\sum_{j=1}^{n_c} x_j A_{ij}}{A} - \frac{B_i}{B}\right)\ln\left(\frac{Z+(1+\sqrt{2})B}{Z-(1+\sqrt{2})B}\right) + \frac{B_i}{Z}\frac{2.5-\eta}{2-3\eta+\eta^2}[x_a(\chi_a-1)+x_r(\chi_r-1)] + 4\ln\chi_i \quad i = a \text{ or } r \tag{C-1}$$

$$\ln \varphi_i = -\ln(Z-B) + \frac{B_i}{B}\left(\frac{B}{Z-B} - \frac{AZ}{Z^2+2BZ-B^2}\right) - \frac{A}{2\sqrt{2}B}\left(\frac{2\sum_{j=1}^{n_c} x_j A_{ij}}{A} - \frac{B_i}{B}\right)\ln\left(\frac{Z+(1+\sqrt{2})B}{Z-(1+\sqrt{2})B}\right), \quad i \neq a \text{ and } r \tag{C-2}$$

where $\varphi_i = f_i/(x_i p)$. To calculate the derivatives of φ_i with respect to composition, we consider the following chain rule:

$$\frac{\partial \ln \varphi_i}{\partial x_j} = \frac{\partial F(\ln \varphi_i)}{\partial Z}\frac{\partial Z}{\partial x_j} + \frac{\partial F(\ln \varphi_i)}{\partial A}\frac{\partial A}{\partial x_j} + \frac{\partial F(\ln \varphi_i)}{\partial B}\frac{\partial B}{\partial x_j} + \frac{\partial F(\ln \varphi_i)}{\partial x_j} + \frac{\partial F(\ln \varphi_i)}{\partial \chi_a}\frac{\partial \chi_a}{\partial x_j} + \frac{\partial F(\ln \varphi_i)}{\partial \chi_r}\frac{\partial \chi_r}{\partial x_j} + \frac{\partial F(\ln \varphi_i)}{\partial \eta}\frac{\partial \eta}{\partial x_j} \tag{C-3}$$

The terms in the above equation are obtained from

$$\frac{\partial F(\ln \varphi_i)}{\partial Z} = -\frac{1}{(Z-B)} + \frac{B_i}{B}\left(-\frac{B}{(Z-B)^2} + \frac{2AB(B-Z)}{(Z^2+2BZ-B^2)^2}\right) + \frac{2\sum_{j=1}^{n_c} x_j A_{ij}}{Z^2+2BZ-B^2} - \frac{B_i}{Z^2}\frac{2.5-\eta}{2-3\eta+\eta^2}[x_a(\chi_a-1)+x_r(\chi_r-1)] \quad i = a \text{ or } r \tag{C-4}$$

$$\frac{\partial F(\ln \varphi_i)}{\partial Z} = -\frac{1}{(Z-B)} + \frac{B_i}{B}\left(-\frac{B}{(Z-B)^2} + \frac{2AB(B-Z)}{(Z^2+2BZ-B^2)^2}\right) + \frac{2\sum_{j=1}^{n_c} x_j A_{ij}}{Z^2+2BZ-B^2} \quad i \neq a \text{ and } r \tag{C-5}$$

$$\frac{\partial F(\ln \varphi_i)}{\partial A} = \frac{B_i}{B}\left(\frac{AZ}{Z^2+2BZ-B^2}\right) + \frac{AB_i}{2\sqrt{2}B^2}\ln\left(\frac{Z+(1+\sqrt{2})B}{Z-(1+\sqrt{2})B}\right) \tag{C-6}$$

$$\frac{\partial F(\ln \varphi_i)}{\partial B} = \frac{1}{(Z-B)} - \frac{B_i}{B^2}\left(\frac{B}{Z-B} - \frac{2AZ}{Z^2+2BZ-B^2}\right) + \frac{B_i}{B}\left(\frac{Z}{(Z-B)^2} + \frac{2AZ(Z-B)}{(Z^2+2BZ-B^2)^2}\right) + \left(\frac{\sum_{j=1}^{n_c} x_j A_{ij}}{\sqrt{2}B^2} - \frac{AB_i}{\sqrt{2}B^2}\right)\ln\left(\frac{Z+(1+\sqrt{2})B}{Z-(1+\sqrt{2})B}\right) - \frac{Z}{B}\frac{2\sum_{j=1}^{n_c} x_j A_{ij}}{Z^2+2BZ-B^2} \quad i = a \text{ or } r, \quad j = 1, \ldots, n_c - 1 \tag{C-7}$$

$$\frac{\partial F(\ln \varphi_i)}{\partial x_j} = \frac{A_{in_c} - A_{ij}}{\sqrt{2}B}\ln\left(\frac{Z+(1+\sqrt{2})B}{Z-(1+\sqrt{2})B}\right) + \frac{B_i}{Z}\frac{2.5-\eta}{2-3\eta+2\eta^2}\chi_i \quad i = a \text{ or } r, \quad j = 1, \ldots, n_c - 1 \tag{C-8}$$

$$\frac{\partial F(\ln \varphi_i)}{\partial x_j} = \frac{A_{in_c} - A_{ij}}{\sqrt{2}B}\ln\left(\frac{Z+(1+\sqrt{2})B}{Z-(1+\sqrt{2})B}\right) \quad i \neq a \text{ and } r, \quad j = 1, \ldots, n_c - 1 \tag{C-9}$$

$$\frac{\partial F(\ln \varphi_i)}{\partial \chi_k} = \frac{B_i}{Z}\frac{2.5-\eta}{2-3\eta+\eta^2}x_k + \frac{4}{\chi_k} \quad i = a \text{ or } r, \quad k = a \text{ or } r \tag{C-10}$$

$$\frac{\partial F(\ln \varphi_i)}{\partial \chi_k} = 0 \quad i \neq a \text{ and } r, \quad k = a \text{ or } r \tag{C-11}$$

$$\frac{\partial F(\ln \varphi_i)}{\partial \eta} = \frac{B_i}{Z}\frac{5.5-5\eta+\eta^2}{(2-3\eta+\eta^2)^2}[x_a(\chi_a-1)+x_r(\chi_r-1)] \quad i = a \text{ or } r \tag{C-12}$$

$$\frac{\partial F(\ln \varphi_i)}{\partial \eta} = 0 \quad i \neq a \text{ and } r \tag{C-13}$$

$$\frac{\partial A}{\partial x_j} = 2\sum_{i=1}^{n_c} x_i(A_{ij} - A_{in_c}) \tag{C-14}$$

$$\frac{\partial B}{\partial x_j} = B_j - B_{n_c} \tag{C-15}$$

The terms $\partial Z/\partial x_j$, $\partial \chi_a/\partial x_j$, and $\partial \chi_r/\partial x_j$ can be obtained from Appendix D. To calculate $(\partial f_{i,\alpha}/\partial p)_{\mathbf{n}_\alpha}$, we use the following equation:

$$\left(\frac{\partial f_{i,\alpha}}{\partial p}\right)_{\mathbf{n}_\alpha} = \frac{f_{i,\alpha}}{RT}\left[\frac{Z_\alpha RT}{p} + \frac{n_\alpha RT}{p}\left(\frac{\partial Z_\alpha}{\partial n_{k,\alpha}}\right)_{T,p,\mathbf{n}_{\alpha,k}}\right] \tag{C-16}$$

APPENDIX D: EXPRESSIONS OF $(\partial Z/\partial n_k)_{T,n_k}$ AND $(\partial Z/\partial p)_{T,n_j}$ FROM CPA-EOS

In this Appendix, the expressions to calculate $(\partial Z/\partial n_k)_{T,n_k}$ and $(\partial Z/\partial p)_{T,n_j}$ using the CPA-EOS are presented. From the CPA-EOS, we have

$$Z = \frac{Z}{Z-B} - \frac{AZ}{Z^2+2BZ-B^2} + \frac{4+4\eta-2\eta^2}{2-3\eta+\eta^2}[x_a(\chi_a-1)+x_r(\chi_r-1)] \quad \alpha = g, o, a \tag{D-1}$$

To calculate the derivative of Z with respect to composition, we have

$$\frac{\partial Z}{\partial x_k} = \frac{\partial F(Z)}{\partial Z}\frac{\partial Z}{\partial x_k} + \frac{\partial F(Z)}{\partial A}\frac{\partial A}{\partial x_k} + \frac{\partial F(Z)}{\partial B}\frac{\partial B}{\partial x_k} + \frac{\partial F(Z)}{\partial x_k} + \frac{\partial F(Z)}{\partial \chi_a}\frac{\partial \chi_a}{\partial x_k} + \frac{\partial F(Z)}{\partial \chi_r}\frac{\partial \chi_r}{\partial x_k} + \frac{\partial F(Z)}{\partial \eta}\frac{\partial \eta}{\partial x_k} \tag{D-2}$$

Using the chain rule, we have the following equations for $\partial \chi_a/\partial x_k$, $\partial \chi_r/\partial x_k$, and $\partial \eta/\partial x_k$:

$$\frac{\partial \chi_a}{\partial x_k} = \frac{\partial F(\chi_a)}{\partial Z}\frac{\partial Z}{\partial x_k} + \frac{\partial F(\chi_a)}{\partial x_k} + \frac{\partial F(\chi_a)}{\partial \chi_a}\frac{\partial \chi_a}{\partial x_k} + \frac{\partial F(\chi_a)}{\partial \chi_r}\frac{\partial \chi_r}{\partial x_k} + \frac{\partial F(\chi_a)}{\partial \Delta^{aa}}\frac{\partial \Delta^{aa}}{\partial \eta}\frac{\partial \eta}{\partial x_k} + \frac{\partial F(\chi_a)}{\partial \Delta^{ar}}\frac{\partial \Delta^{ar}}{\partial \eta}\frac{\partial \eta}{\partial x_k} \tag{D-3}$$

$$\frac{\partial \chi_r}{\partial x_k} = \frac{\partial F(\chi_r)}{\partial Z}\frac{\partial Z}{\partial x_k} + \frac{\partial F(\chi_r)}{\partial x_k} + \frac{\partial F(\chi_r)}{\partial \chi_a}\frac{\partial \chi_a}{\partial x_k} + \frac{\partial F(\chi_a)}{\partial \Delta^{ar}}\frac{\partial \Delta^{ar}}{\partial \eta}\frac{\partial \eta}{\partial x_k} \tag{D-4}$$

DOI: 10.1021/acs.energyfuels.5b02944
Energy Fuels 2016, 30, 3306−3319

$$\frac{\partial \eta}{\partial x_k} = \frac{\partial F(\eta)}{\partial Z}\frac{\partial Z}{\partial x_k} + \frac{\partial F(\eta)}{\partial B}\frac{\partial B}{\partial x_k} \tag{D-5}$$

We define f_1, f_2, and f_3 as

$$f_1 = \frac{\partial F(\chi_a)}{\partial Z} + \frac{\partial F(\chi_a)}{\partial \chi_r}\frac{\partial \chi_r}{\partial Z} + \frac{\partial F(\chi_a)}{\partial \chi_r}\frac{\partial F(\chi_r)}{\partial \Delta^{aa}}\frac{\partial \Delta^{aa}}{\partial \eta}\frac{\partial F(\eta)}{\partial Z} + \frac{\partial F(\chi_a)}{\partial \chi_r}\frac{\partial F(\chi_r)}{\partial \Delta^{ar}}\frac{\partial \Delta^{ar}}{\partial \eta}\frac{\partial F(\eta)}{\partial Z} + \frac{\partial F(\chi_a)}{\partial \Delta^{aa}}\frac{\partial \Delta^{aa}}{\partial \eta}\frac{\partial F(\eta)}{\partial Z} + \frac{\partial F(\chi_a)}{\partial \Delta^{ar}}\frac{\partial \Delta^{ar}}{\partial \eta}\frac{\partial F(\eta)}{\partial Z} \tag{D-6}$$

$$f_2 = \frac{\partial B}{\partial x_k}\left(\frac{\partial F(\chi_a)}{\partial \chi_r}\frac{\partial F(\chi_r)}{\partial \Delta^{aa}}\frac{\partial \Delta^{aa}}{\partial \eta}\frac{\partial F(\eta)}{\partial Z} + \frac{\partial F(\chi_a)}{\partial \chi_r}\frac{\partial F(\chi_r)}{\partial \Delta^{ar}}\frac{\partial \Delta^{ar}}{\partial \eta}\frac{\partial F(\eta)}{\partial Z} + \frac{\partial F(\chi_a)}{\partial \Delta^{aa}}\frac{\partial \Delta^{aa}}{\partial \eta}\frac{\partial F(\eta)}{\partial Z} + \frac{\partial F(\chi_r)}{\partial \Delta^{ar}}\frac{\partial \Delta^{ar}}{\partial \eta}\frac{\partial F(\eta)}{\partial Z}\right) + \frac{\partial F(\chi_a)}{\partial x_k} + \frac{\partial F(\chi_a)}{\partial \chi_r}\frac{\partial \chi_r}{\partial x_k} \tag{D-7}$$

$$f_3 = 1 - \frac{\partial F(\chi_a)}{\partial \chi_a} - \frac{\partial F(\chi_a)}{\partial \chi_r}\frac{\partial F(\chi_r)}{\partial \chi_a} \tag{D-8}$$

If we substitute eqs D-4 and D-5 into eq D-3, using the above definitions, we obtain

$$\frac{\partial \chi_a}{\partial x_k} = \frac{f_1}{f_3}\frac{\partial Z}{\partial x_k} + \frac{f_2}{f_3} \tag{D-9}$$

We define f_4 and f_5 as

$$f_4 = \frac{\partial F(\chi_r)}{\partial Z} + \frac{f_1}{f_3}\frac{\partial F(\chi_r)}{\partial \chi_a} + \frac{\partial F(\chi_r)}{\partial \Delta^{aa}}\frac{\partial \Delta^{aa}}{\partial \eta}\frac{\partial F(\eta)}{\partial Z} + \frac{\partial F(\chi_r)}{\partial \Delta^{ar}}\frac{\partial \Delta^{ar}}{\partial \eta}\frac{\partial F(\eta)}{\partial Z} \tag{D-10}$$

$$f_5 = \frac{\partial F(\chi_r)}{\partial x_k} + \frac{f_2}{f_3}\frac{\partial F(\chi_r)}{\partial \chi_a} + \frac{\partial F(\chi_r)}{\partial \Delta^{ar}}\frac{\partial F(\Delta^{ar})}{\partial \eta}\frac{\partial F(\eta)}{\partial B}\frac{\partial B}{\partial x_k} \tag{D-11}$$

Then, substituting eqs D-5 and) into eq D-4, we have

$$\frac{\partial \chi_r}{\partial x_k} = f_4\frac{\partial Z}{\partial x_k} + f_5 \tag{D-12}$$

We define f_6 and f_7 as

$$f_6 = \frac{\partial F(Z)}{\partial A}\frac{\partial A}{\partial x_k} + \left(\frac{\partial F(Z)}{\partial B} + \frac{\partial F(Z)}{\partial \eta}\frac{\partial \eta}{\partial B}\right)\frac{\partial B}{\partial x_k} + \frac{\partial F(Z)}{\partial x_k} + \frac{f_2}{f_3}\frac{\partial F(Z)}{\partial \chi_a} + f_5\frac{\partial F(Z)}{\partial \chi_r} \tag{D-13}$$

$$f_7 = 1 - \frac{\partial F(Z)}{\partial Z} - \frac{f_1}{f_3}\frac{\partial F(Z)}{\partial \chi_a} - f_4\frac{\partial F(Z)}{\partial \chi_r}\frac{\partial F(Z)}{\partial \eta}\frac{\partial F(\eta)}{\partial Z} \tag{D-14}$$

If we substitute eqs D-5, D-9, and D-12 into eq D-2, using the above definitions, we obtain

$$\frac{\partial Z}{\partial x_k} = \frac{f_6}{f_7} \tag{D-15}$$

$$\frac{\partial \eta}{\partial x_k} = \frac{f_6}{f_7}\frac{\partial f(\eta)}{\partial Z} + \frac{\partial f(\eta)}{\partial B}\frac{\partial B}{\partial x_k} \tag{D-16}$$

The partial derivatives in the above equations are given by

$$\frac{\partial F(Z)}{\partial Z} = \frac{B}{(Z-B)^2} + \frac{A(Z^2+B^2)}{(Z^2+2BZ-B^2)^2} \tag{D-17}$$

$$\frac{\partial F(Z)}{\partial A} = -\frac{Z}{Z^2+2BZ-B^2} \tag{D-18}$$

$$\frac{\partial F(Z)}{\partial B} = \frac{Z}{(Z-B)^2} + \frac{2AZ(Z-B)}{(Z^2+2BZ-B^2)^2} \tag{D-19}$$

$$\frac{\partial F(Z)}{\partial x_k} = \frac{4+4\eta-2\eta^2}{2-3\eta+\eta^2}(\chi_k - 1) \qquad k = a \text{ or } r \tag{D-20}$$

$$\frac{\partial F(Z)}{\partial x_k} = 0 \qquad k \neq a \text{ and } r \tag{D-21}$$

$$\frac{\partial F(Z)}{\partial \chi_k} = x_k\frac{4+4\eta-2\eta^2}{2-3\eta+\eta^2} \qquad k = a \text{ or } r \tag{D-22}$$

$$\frac{\partial F(Z)}{\partial \eta} = \frac{20-16\eta+2\eta^2}{(2-3\eta+\eta^2)^2}[x_a(\chi_a - 1) + x_r(\chi_r - 1)] \tag{D-23}$$

$$\frac{\partial A}{\partial x_k} = 2\sum_{i=1}^{n_c} x_i(A_{ik} - A_{in_c}) \tag{D-24}$$

$$\frac{\partial B}{\partial x_k} = B_k - B_{n_c} \tag{D-25}$$

$$\frac{\partial F(\chi_a)}{\partial Z} = \frac{N_a x_{a,\alpha}\chi_{a,\alpha}\Delta^{aa} + N_r x_{r,\alpha}\chi_{r,\alpha}\Delta^{ar}}{(Z + N_a x_\alpha \chi_a \Delta^{aa} + N_r x_r \chi_r \Delta^{ar})^2} \tag{D-26}$$

$$\frac{\partial F(\chi_a)}{\partial x_k} = -\frac{N_k \chi_k \Delta^{ak} Z}{(Z + N_a x_\alpha \chi_a \Delta^{aa} + N_r x_r \chi_r \Delta^{ar})^2} \qquad k = a \text{ or } r \tag{D-27}$$

$$\frac{\partial F(\chi_a)}{\partial x_k} = 0 \qquad k \neq a \text{ and } r \tag{D-28}$$

$$\frac{\partial F(\chi_a)}{\partial \chi_a} = -\frac{N_a x_a \Delta^{aa} Z}{(Z + N_a x_\alpha \chi_a \Delta^{aa} + N_r x_r \chi_r \Delta^{ar})^2} \tag{D-29}$$

$$\frac{\partial F(\chi_a)}{\partial \chi_r} = -\frac{N_r x_r \Delta^{ar} Z}{(Z + N_a x_\alpha \chi_a \Delta^{aa} + N_r x_r \chi_r \Delta^{ar})^2} \tag{D-30}$$

$$\frac{\partial F(\chi_a)}{\partial \Delta^{aa}} = -\frac{N_a x_\alpha \chi_a Z}{(Z + N_a x_\alpha \chi_a \Delta^{aa} + N_r x_r \chi_r \Delta^{ar})^2} \tag{D-31}$$

$$\frac{\partial F(\chi_a)}{\partial \Delta^{ar}} = -\frac{N_r x_r \chi_r Z}{(Z + N_a x_\alpha \chi_a \Delta^{aa} + N_r x_r \chi_r \Delta^{ar})^2} \tag{D-32}$$

$$\frac{\partial F(\chi_r)}{\partial Z} = -\frac{N_a x_\alpha \chi_a \Delta^{ar}}{(Z + N_a x_\alpha \chi_a \Delta^{ar})^2} \tag{D-33}$$

DOI: 10.1021/acs.energyfuels.5b02944
Energy Fuels 2016, 30, 3306−3319

$$\frac{\partial F(\chi_r)}{\partial x_k} = -\frac{N_a \chi_a \Delta^{ar} Z}{(Z + N_a x_a \chi_a \Delta^{ar})^2} \qquad k = a \tag{D-34}$$

$$\frac{\partial F(\chi_r)}{\partial x_k} = 0 \qquad k \neq a \tag{D-35}$$

$$\frac{\partial F(\chi_r)}{\partial \chi_a} = -\frac{N_a x_a \Delta^{ar} Z}{(Z + N_a x_a \chi_a \Delta^{ar})^2} \tag{D-36}$$

$$\frac{\partial F(\chi_r)}{\partial \Delta^{ar}} = -\frac{N_a x_a \chi_a Z}{(Z + N_a x_a \chi_a \Delta^{ar})^2} \tag{D-37}$$

$$\frac{\partial F(\eta)}{\partial Z} = -\frac{B}{4Z^2} \tag{D-38}$$

$$\frac{\partial F(\eta)}{\partial B} = \frac{1}{4Z} \tag{D-39}$$

$$\frac{\partial \Delta^{ij}}{\partial \eta} = \frac{2.5 - \eta}{(1-\eta)^4} \kappa_{ij} b_{ij} \left[\exp\left(\frac{\varepsilon_{ij}}{k_b T} \right) - 1 \right] \qquad i = a, \quad j = a \text{ or } r \tag{D-40}$$

To calculate the derivative of Z with respect to pressure, we have

$$\frac{\partial Z}{\partial p} = \frac{\partial F(Z)}{\partial Z}\frac{\partial Z}{\partial p} + \frac{\partial F(Z)}{\partial A}\frac{\partial A}{\partial p} + \frac{\partial F(Z)}{\partial B}\frac{\partial B}{\partial p} + \frac{\partial F(Z)}{\partial \chi_a}\frac{\partial \chi_a}{\partial p} + \frac{\partial F(Z)}{\partial \chi_r}\frac{\partial \chi_r}{\partial p} + \frac{\partial F(Z)}{\partial \eta}\frac{\partial \eta}{\partial p} \tag{D-41}$$

Using the chain rule, we have the following equations for $\partial\chi_a/\partial p$, $\partial\chi_r/\partial p$, and $\partial\eta/\partial p$:

$$\frac{\partial \chi_a}{\partial p} = \frac{\partial F(\chi_a)}{\partial Z}\frac{\partial Z}{\partial p} + \frac{\partial F(\chi_a)}{\partial \chi_a}\frac{\partial \chi_a}{\partial p} + \frac{\partial F(\chi_a)}{\partial \chi_r}\frac{\partial \chi_r}{\partial p} + \frac{\partial F(\chi_a)}{\partial \Delta^{aa}}\frac{\partial \Delta^{aa}}{\partial \eta}\frac{\partial \eta}{\partial p} + \frac{\partial F(\chi_a)}{\partial \Delta^{ar}}\frac{\partial \Delta^{ar}}{\partial \eta}\frac{\partial \eta}{\partial p} \tag{D-42}$$

$$\frac{\partial \chi_r}{\partial p} = \frac{\partial F(\chi_r)}{\partial Z}\frac{\partial Z}{\partial p} + \frac{\partial F(\chi_r)}{\partial \chi_a}\frac{\partial \chi_a}{\partial p} + \frac{\partial F(\chi_a)}{\partial \Delta^{ar}}\frac{\partial \Delta^{ar}}{\partial \eta}\frac{\partial \eta}{\partial p} \tag{D-43}$$

$$\frac{\partial \eta}{\partial p} = \frac{\partial F(\eta)}{\partial Z}\frac{\partial Z}{\partial p} + \frac{\partial F(\eta)}{\partial B}\frac{\partial B}{\partial p} \tag{D-44}$$

$$\frac{\partial \Delta^{ij}}{\partial p} = \frac{\partial F(\Delta^{ij})}{\partial \eta}\frac{\partial \eta}{\partial p} \qquad i = a, \; j = a \text{ or } r \tag{D-45}$$

We define g_1, g_2, and g_3 as

$$g_1 = f_1 \tag{D-46}$$

$$g_2 = \frac{\partial B}{\partial p}\left(\frac{\partial F(\chi_a)}{\partial \chi_r}\frac{\partial F(\chi_r)}{\partial \Delta^{aa}}\frac{\partial \Delta^{aa}}{\partial \eta}\frac{\partial F(\eta)}{\partial Z} + \frac{\partial F(\chi_a)}{\partial \chi_r}\frac{\partial F(\chi_r)}{\partial \Delta^{ar}}\frac{\partial \Delta^{ar}}{\partial \eta}\frac{\partial F(\eta)}{\partial Z} + \frac{\partial F(\chi_a)}{\partial \Delta^{aa}}\frac{\partial \Delta^{aa}}{\partial \eta}\frac{\partial F(\eta)}{\partial Z} + \frac{\partial F(\chi_r)}{\partial \Delta^{ar}}\frac{\partial \Delta^{ar}}{\partial \eta}\frac{\partial F(\eta)}{\partial Z} \right) \tag{D-47}$$

$$g_3 = f_3 \tag{D-48}$$

If we substitute eqs D-43, D-44, and D-45 into eq D-42, using the above definitions, we can obtain

$$\frac{\partial \chi_a}{\partial p} = \frac{g_1}{g_3}\frac{\partial Z}{\partial p} + \frac{g_2}{g_3} \tag{D-49}$$

Substituting eqs D-44, D-45, and D-49 into eq D-43 and defining g_4 and g_5 as

$$g_4 = f_4 \tag{D-50}$$

$$g_5 = \frac{g_2}{g_3}\frac{\partial F(\chi_r)}{\partial \chi_a} + \frac{\partial F(\chi_r)}{\partial \Delta^{ar}}\frac{\partial F(\Delta^{ar})}{\partial \eta}\frac{\partial F(\eta)}{\partial B}\frac{\partial B}{\partial p} \tag{D-51}$$

we have

$$\frac{\partial \chi_r}{\partial p} = g_4\frac{\partial Z}{\partial p} + g_5 \tag{D-52}$$

We define g_6 and g_7 as

$$g_6 = \frac{\partial F(Z)}{\partial A}\frac{\partial A}{\partial p} + \left(\frac{\partial F(Z)}{\partial B} + \frac{\partial F(Z)}{\partial \eta}\frac{\partial \eta}{\partial B} \right)\frac{\partial B}{\partial p} + \frac{g_2}{g_3}\frac{\partial F(Z)}{\partial \chi_a} + g_5\frac{\partial F(Z)}{\partial \chi_r} \tag{D-53}$$

$$g_7 = f_7 \tag{D-54}$$

If we substitute eqs D-44, D-45, and D-49 into eq D-41, using the above definitions, we obtain

$$\frac{\partial Z}{\partial p} = \frac{g_6}{g_7} \tag{D-55}$$

$$\frac{\partial \eta}{\partial p} = \frac{g_6}{g_7}\frac{\partial f(\eta)}{\partial Z} + \frac{\partial f(\eta)}{\partial B}\frac{\partial B}{\partial p} \tag{D-56}$$

The partial derivatives in the above equations are defined previously except for $\partial A/\partial p$ and $\partial B/\partial p$ given by

$$\frac{\partial A}{\partial p} = \frac{A}{p} \tag{D-57}$$

$$\frac{\partial B}{\partial p} = \frac{B}{p} \tag{D-58}$$

AUTHOR INFORMATION

Corresponding Author

*Phone: (979)8626483. Fax: (979)8451307. E-mail: hadi.nasrabadi@tamu.edu.

Notes

The authors declare no competing financial interest.

ACKNOWLEDGMENTS

This research is supported by the Qatar National Research Fund under Grant NPRP 09-1050-2-405. This support is greatly appreciated. We also thank Dr. Zhidong Li, currently with ExxonMobil, for helpful technical discussions.

NOMENCLATURE

A = Peng−Robinson equation of state parameter, dimensionless
B = Peng−Robinson equation of state parameter, dimensionless
c = overall molar density, mol/m^3
c_f = total fluid compressibility, 1/Pa

DOI: 10.1021/acs.energyfuels.5b02944
Energy Fuels 2016, 30, 3306−3319

F_i = the sink or source term for component i, mol/(s·m^3)
$f_{i,\alpha}$ = fugacity of component i in phase α, Pa
g = acceleration of gravity, m^2/s
k = absolute permeability, m^2
k_b = Boltzmann constant, J/K
$k_{r\alpha}$ = relative permeability of phase α, dimensionless
M_i = molecular weight of component i, g/mol
N_i = number of association sites of molecule i
n = number of moles
n_c = number of components
p = pressure, Pa
p_c = critical pressure, Pa
R = universal gas constant, J/(K·mol)
T = temperature, K
T_c = critical temperature, K
u_α = phase velocity, m/s
V = volume, m^3
$\overline{v_i}$ = total partial molar volume of component i, m^3/mol
$x_{i,\alpha}$ = mole fraction of component i in phase α, dimensionless
Z_α = compressibility factor of phase α
z_i = overall composition of component i, dimensionless

Greek Letters

β_α = molar fractions of phase α, dimensionless
Δ^{ij} = association strength between site i and site j, dimensionless
ε_{ij} = energy parameter, J
η = cubic-plus-association equation of state parameter, dimensionless
κ_{ij} = association volume, dimensionless
μ_α = viscosity of phase α, kg/(m·s)
ρ_α = mass density of phase α, kg/m^3
ϕ = porosity, dimensionless
$\varphi_{i,\alpha}$ = fugacity coefficient of component i in phase α, dimensionless
χ_i = mole fractions of component i not bonded at one of the association sites, dimensionless

Subscripts

a = asphaltene-rich liquid phase
g = gas phase
i = component
o = hydrocarbon-rich liquid phase
r = resins/aromatics
α = phase

REFERENCES

(1) Firoozabadi, A. *Thermodynamics of hydrocarbon reservoirs*; McGraw-Hill: New York, 1999.
(2) Buckley, J. S. *SPE Advanced Technology Series* **1995**, *3* (1), 53−59.
(3) Kamath, V. A.; Yang, J.; Sharma, G. D. *Effect of Asphaltene Deposition on Dynamic Displacements of Oil by Water*, SPE Western Regional Meeting, SPE-26046-MS, Anchorage, AK, USA, May 26−28, 1993; Society of Petroleum Engineers: Richardson, TX, USA, 1993; DOI: 10.2118/26046-MS.
(4) Clementz, D. M. *Alteration of Rock Properties by Adsorption of Petroleum Heavy Ends: Implications for Enhanced Oil Recovery*, SPE Enhanced Oil Recovery Symposium, SPE-10683-MS, Tulsa, OK, USA, Apr. 4−7, 1982; Society of Petroleum Engineers: Richardson, TX, USA, 1982; DOI: 10.2118/10683-MS.
(5) Hirschberg, A.; Dejong, L. N. J.; Schipper, B. A.; Meijer, J. G. *SPEJ, Soc. Pet. Eng. J.* **1984**, *24* (3), 283−293.
(6) Wang, J. X.; Buckley, J. S. *Energy Fuels* **2001**, *15* (5), 1004−1012.
(7) Correra, S. *Pet. Sci. Technol.* **2004**, *22* (7−8), 943−959.
(8) Correra, S.; Merino-Garcia, D. *Energy Fuels* **2007**, *21* (3), 1243−1247.
(9) Jamshidnezhad, M. *J. Jpn. Pet. Inst.* **2008**, *51* (4), 217−224.
(10) Kraiwattanawong, K.; Fogler, H. S.; Gharfeh, S. G.; Singh, P.; Thomason, W. H.; Chavadej, S. *Energy Fuels* **2007**, *21* (3), 1248−1255.
(11) Akbarzadeh, K.; Alboudwarej, H.; Svrcek, W. Y.; Yarranton, H. W. *Fluid Phase Equilib.* **2005**, *232* (1−2), 159−170.
(12) Nikookar, M.; Pazuki, G. R.; Omidkhah, M. R.; Sahranavard, L. *Fuel* **2008**, *87* (1), 85−91.
(13) Alboudwarej, H.; Akbarzadeh, K.; Beck, J.; Svrcek, W. Y.; Yarranton, H. W. *AIChE J.* **2003**, *49* (11), 2948−2956.
(14) Gupta, A. K. *A model for asphaltene flocculation using an equation of state*. M.Sc. thesis, University of Calgary, Canada, 1986.
(15) Godbole, S. P.; Thele, K. J.; Reinbold, E. W. *SPE Reservoir Eng.* **1995**, *10* (2), 101−108.
(16) Nghiem, L. X.; Hassam, M. S.; Nutakki, R.; George, A. E. D. *Efficient Modeling of Asphaltene Precipitation*, SPE Annual Technical Conference and Exhibition, SPE-26642-MS, Houston, TX, USA, Oct. 3−6, 1993; Society of Petroleum Engineers: Richardson, TX, USA, 1993; DOI: 10.2118/26642-MS.
(17) Kohse, B. F.; Nghiem, L. X.; Maeda, H.; Ohno, K. *Modeling Phase Behaviour Including the Effect of Pressure and Temperature on Asphaltene Precipitation*, SPE Asia Pacific Oil and Gas Conference and Exhibition, SPE-64465-MS, Brisbane, Australia, Oct. 16−18, 2000; Society of Petroleum Engineers: Richardson, TX, USA, 2000; DOI: 10.2118/64465-MS.
(18) Vafaie-Sefti, M.; Mousavi-Dehghani, S. A.; Mohammad-Zadeh, M. *Fluid Phase Equilib.* **2003**, *206* (1−2), 1−11.
(19) Leontaritis, K. J.; Mansoori, G. A. *Asphaltene Flocculation During Oil Production and Processing: A Thermodynamic Collodial Model*, SPE International Symposium on Oilfield Chemistry, SPE-16258-MS, San Antonio, TX, USA, Feb. 4−6, 1987; Society of Petroleum Engineers: Richardson, TX, USA, 1987; DOI: 10.2118/16258-MS.
(20) Victorov, A. I.; Firoozabadi, A. *AIChE J.* **1996**, *42* (6), 1753−1764.
(21) Pan, H. Q.; Firoozabadi, A. *SPE Prod. Facil.* **2000**, *15* (1), 58−65.
(22) Pan, H. Q.; Firoozabadi, A. *AIChE J.* **2000**, *46* (2), 416−426.
(23) Wu, J.; Prausnitz, J. M.; Firoozabadi, A. *AIChE J.* **1998**, *44* (5), 1188−1199.
(24) Wu, J.; Prausnitz, J. M.; Firoozabadi, A. *AIChE J.* **2000**, *46* (1), 197−209.
(25) Buenrostro-Gonzalez, E.; Lira-Galeana, C.; Gil-Villegas, A.; Wu, J. *AIChE J.* **2004**, *50* (10), 2552−2570.
(26) Gonzalez, D. L.; Vargas, F. M.; Hirasaki, G. J.; Chapman, W. G. *Energy Fuels* **2008**, *22* (2), 757−762.
(27) Ting, P. D.; Hirasaki, G. J.; Chapman, W. G. *Pet. Sci. Technol.* **2003**, *21* (3−4), 647−661.
(28) Vargas, F. M.; Gonzalez, D. L.; Hirasaki, G. J.; Chapman, W. G. *Energy Fuels* **2009**, *23* (3), 1140−1146.
(29) Li, Z.; Firoozabadi, A. *Energy Fuels* **2010**, *24* (5), 2956−2963.
(30) Mohebbinia, S.; Sepehrnoori, K.; Johns, R. T.; Kazemi Nia Korrani, A. *Simulation of Asphaltene Precipitation during Gas Injection Using PC-SAFT EOS*, SPE Annual Technical Conference and Exhibition, SPE-170697-MS, Amsterdam, The Netherlands, Oct. 27−29, 2014; Society of Petroleum Engineers: Richardson, TX, USA, 2014; DOI: 10.2118/170697-MS.
(31) Li, Z.; Firoozabadi, A. *AIChE J.* **2009**, *55* (7), 1803−1813.
(32) Peng, D. Y.; Robinson, D. B. *Ind. Eng. Chem. Fundam.* **1976**, *15* (1), 59−64.
(33) Jindrová, T.; Mikyška, J.; Firoozabadi, A. *Energy Fuels* **2016**, *30* (1), 515−525.
(34) Zhang, X.; Pedrosa, N.; Moorwood, T. *Energy Fuels* **2012**, *26* (5), 2611−2620.
(35) Hoteit, H.; Firoozabadi, A. *SPE Journal* **2009**, *14* (2), 323−337.
(36) Moortgat, J. *Adv. Water Resour.* **2016**, *89*, 53−66.
(37) Pedersen, K. S.; Fredenslund, A. *Chem. Eng. Sci.* **1987**, *42* (1), 182−186.
(38) Stone, H. L. *JPT, J. Pet. Technol.* **1970**, *22* (2), 214−218.
(39) Acs, G.; Doleschall, S.; Farkas, E. *SPEJ, Soc. Pet. Eng. J.* **1985**, *25* (4), 543−553.
(40) Watts, J. W. *SPE Reservoir Eng.* **1986**, *1* (3), 243−252.
(41) Hoteit, H.; Firoozabadi, A. *SPE Journal* **2006**, *11* (1), 19−34.

DOI: 10.1021/acs.energyfuels.5b02944
Energy Fuels 2016, 30, 3306−3319

(42) Hoteit, H.; Firoozabadi, A. *Water Resour. Res.* **2005**, *41*, W11412.
(43) Hoteit, H.; Firoozabadi, A. *SPE Journal* **2006**, *11* (3), 341−352.
(44) Moortgat, J.; Sun, S.; Firoozabadi, A. *Water Resour. Res.* **2011**, *47* (5), W05511.
(45) Moortgat, J.; Li, Z.; Firoozabadi, A. *Water Resour. Res.* **2012**, *48* (12), W12511.
(46) Shahraeeni, E.; Moortgat, J.; Firoozabadi, A. *Computational Geosciences* **2015**, *19* (4), 899−920.
(47) Moortgat, J.; Firoozabadi, A. *J. Comput. Phys.* **2016**, in press.
(48) Li, Z.; Firoozabadi, A. *SPE Journal* **2012**, *17* (4), 1096−1107.
(49) Hamadou, R.; Khodja, M.; Kartout, M.; Jada, A. *Fuel* **2008**, *87* (10−11), 2178−2185.
(50) Szewczyk, V.; Behar, E. *Fluid Phase Equilib.* **1999**, *158−160* (0), 459−469.
(51) Szewczyk, V.; Thomas, M.; Behar, E. *Rev. Inst. Fr. Pet.* **1998**, *53* (1), 51−58.
(52) Hartono, A.; Kim, I. *Calculation of Vapor-Liquid Equilibria for Methanol-Water Mixture using Cubic-Plus-Association Equation of State*; Norges teknisk-naturvitenskapelige universitet (NTNU): Trondheim, Norway, 2004; http://www.nt.ntnu.no/users/haugwarb/KP8108/Essays/ardi_hartono_and_inna_kim.pdf.
(53) Firoozabadi, A. *Thermodynamics and Applications of Hydrocarbons Energy Production*; McGraw Hill Professional: New York, 2015.
(54) Minssieux, L.; Nabzar, L.; Chauveteau, G.; Longeron, D.; Bensalem, R. *Rev. Inst. Fr. Pet.* **1998**, *53* (3), 313−327.
(55) Papadimitriou, N. I.; Romanos, G. E.; Charalambopoulou, G. C.; Kainourgiakis, M. E.; Katsaros, F. K.; Stubos, A. K. *J. Pet. Sci. Eng.* **2007**, *57* (3−4), 281−293.
(56) Mendoza de la Cruz, J. L.; Argüelles-Vivas, F. J.; Matías-Pérez, V.; Durán-Valencia, C. d. l. A.; López-Ramírez, S. n *Energy Fuels* **2009**, *23* (11), 5611−5625.
(57) Hu, C.; Hartman, R. L. *AIChE J.* **2014**, *60* (10), 3534−3546.
(58) Civan, F. Modeling and Simulation of Formation Damage by Organic Deposition. *Proceedings: First international symposium in colloid chemistry in oil production: Asphaltenes and wax deposition*, ISCOP'95, Rio de Janeiro, Brazil, Nov. 26−29, 1995; Brazil Section, Society of Petroleum Engineers: Rio de Janeiro, Brazil, 1995; pp 102−107.
(59) Wang, S. J.; Civan, F. *J. Energy Resour. Technol.* **2005**, *127* (4), 310−317.
(60) Lawal, K. A.; Vesovic, V.; Boek, E. S. *Energy Fuels* **2011**, *25* (12), 5647−5659.
(61) Li, Z.; Firoozabadi, A. *Energy Fuels* **2010**, *24* (2), 1106−1113.
(62) Srivastava, R. K.; Huang, S. S.; Dyer, S. B.; Mourits, F. M. *J. Can. Pet. Technol.* **1995**, *34* (08), 31−42.
(63) Arbabi, S.; Firoozabadi, A. *SPE Advanced Technology Series* **1995**, *3* (01), 139−145.
(64) Srivastava, R. K.; Huang, S. S.; Dong, M. *SPE Prod. Facil.* **1999**, *14* (4), 235−245.

DOI: 10.1021/acs.energyfuels.5b02944
Energy Fuels 2016, 30, 3306−3319